Behavioral/Cognitive

Attention to Color Sharpens Neural Population Tuning via Feedback Processing in the Human Visual Cortex Hierarchy

Mandy V. Bartsch,[1] Kristian Loewe,[2] Christian Merkel,[2] Hans-Jochen Heinze,[1,2] Mircea A. Schoenfeld,[1,2,3] John K. Tsotsos,[4] and Jens-Max Hopf[1,2]

[1]Leibniz Institute for Neurobiology, 39118 Magdeburg, Germany, [2]Department of Neurology, Otto-von-Guericke University, 39120 Magdeburg, Germany, [3]Kliniken Schmieder Allensbach, 78476 Allensbach, Germany, and [4]Centre for Vision Research, York University, Toronto, Ontario M3J 1P3, Canada

Attention can facilitate the selection of elementary object features such as color, orientation, or motion. This is referred to as feature-based attention and it is commonly attributed to a modulation of the gain and tuning of feature-selective units in visual cortex. Although gain mechanisms are well characterized, little is known about the cortical processes underlying the sharpening of feature selectivity. Here, we show with high-resolution magnetoencephalography in human observers (men and women) that sharpened selectivity for a particular color arises from feedback processing in the human visual cortex hierarchy. To assess color selectivity, we analyze the response to a color probe that varies in color distance from an attended color target. We find that attention causes an initial gain enhancement in anterior ventral extrastriate cortex that is coarsely selective for the target color and transitions within ~100 ms into a sharper tuned profile in more posterior ventral occipital cortex. We conclude that attention sharpens selectivity over time by attenuating the response at lower levels of the cortical hierarchy to color values neighboring the target in color space. These observations support computational models proposing that attention tunes feature selectivity in visual cortex through backward-propagating attenuation of units less tuned to the target.

Key words: color; extrastriate cortex; feature-based attention; MEG; selective tuning

Significance Statement

Whether searching for your car, a particular item of clothing, or just obeying traffic lights, in everyday life, we must select items based on color. But how does attention allow us to select a specific color? Here, we use high spatiotemporal resolution neuromagnetic recordings to examine how color selectivity emerges in the human brain. We find that color selectivity evolves as a coarse to fine process from higher to lower levels within the visual cortex hierarchy. Our observations support computational models proposing that feature selectivity increases over time by attenuating the responses of less-selective cells in lower-level brain areas. These data emphasize that color perception involves multiple areas across a hierarchy of regions, interacting with each other in a complex, recursive manner.

Introduction

Psychophysical observations suggest that feature-based attention (FBA) facilitates performance by increasing the speed and selectivity of discrimination (Lee et al., 1999; Ling et al., 2009; Paltoglou and Neri, 2012). Those beneficial behavioral effects have been attributed to a modulation of neural activity in visual cortical areas specialized for the processing of the attended feature (Corbetta et al., 1990, 1991; Chawla et al., 1999). However, elementary features such as color or orientation are coded at multiple levels of the visual cortical processing hierarchy. In humans, color produces strong fMRI responses in V1, V2, hV4, and ventral occipital (VO) regions (Wade et al., 2002; Liu and Wandell, 2005) and is decodable from the BOLD response in all retinotopic areas of the ventral occipital cortex (V1, V2, V3, and hV4) up to VO-1 (Brouwer and Heeger, 2009). Notably, attending a particular color causes BOLD enhancements at multiple hierarchical levels, including striate and downstream ventral extrastriate areas (Sàenz et al., 2002; McMains et al., 2007). Therefore, the question arises as to the role of multiple FBA modulations arising at different hierarchical levels of cortical representation. Computational models have proposed that a dynamic shift of activity across hierarchical levels is a key component of attentional focus-

Received March 10, 2017; revised Aug. 23, 2017; accepted Aug. 26, 2017.

Author contributions: M.V.B., M.A.S., J.K.T., and J.-M.H. designed research; M.V.B. performed research; K.L., C.M., and H.-J.H. contributed unpublished reagents/analytic tools; M.V.B., K.L., C.M., and J.-M.H. analyzed data; M.V.B., J.K.T., and J.-M.H. wrote the paper.

This work was supported by the Deutsche Forschungsgemeinschaft (Grant SFB779/TPA1). We thank Joseph A. Harris for helpful comments and for editing the manuscript.

The authors declare no competing financial interests.

Correspondence should be addressed to Jens-Max Hopf, Leibniz-Institute for Neurobiology, Brenneckestrasse 6, D-39118 Magdeburg, Germany. E-mail: jens-max.hopf@med.ovgu.de.

DOI:10.1523/JNEUROSCI.0666-17.2017

 0270-6474/17/3710346-12$15.00/0

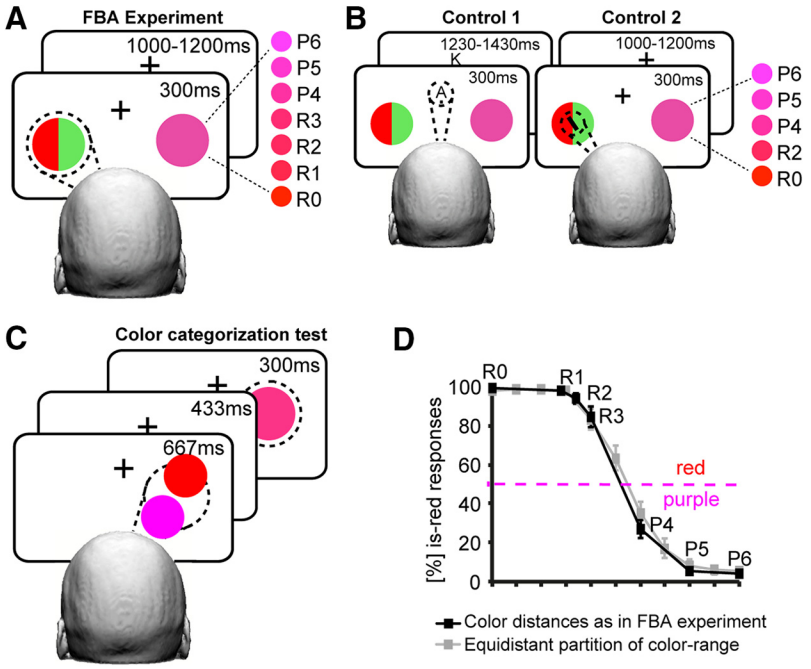

Figure 1. Experimental design. ***A***, FBA experiment. On each trial, the subjects were presented a bicolored target circle in the LVF and a task-irrelevant color probe in the RVF. Subjects were asked to report whether the red half-circle appeared at the left or right side of the circle. The probe in the RVF varied randomly between different red and purple hues spanning from focal red (R0) to focal purple (P6). The brain response elicited by the color probe was analyzed as a function of color distance to the target red. ***B***, Control experiments. Left, Control Experiment 1: Attention was drawn away from the color target by presenting an RSVP stream at fixation. Subjects ignored the colored circles and reported whether the RSVP stream contained the character "0" (present in 50% of the trials) or not. Right, Control Experiment 2: Subjects fixated the central cross, ignored the colored circles, and reported whether the small black bar superimposed on the target circle was tilted clockwise or counterclockwise from vertical. ***C***, Behavioral color categorization test. While fixating subjects covertly attended to the RVF, each trial started with the presentation of two circles (drawn in R0 and P6), which served as a color reference, before a unicolored circle was presented for 300 ms. Subjects reported whether the circle was a red or a purple. ***D***, Behavioral data of the color categorization test. Error bars indicate SEM. Independent of the partition of the color range, the subjects set the categorical border somewhere between R3 (classified as red) and P4 (classified as purple).

ing in space (Tsotsos, 1990; Olshausen et al., 1993; Salinas and Abbott, 1997) and essentially accounts for the sharpening of spatial tuning (Tsotsos et al., 1995; Cutzu and Tsotsos, 2003; Tsotsos et al., 2008; Tsotsos, 2011). Selection across hierarchical levels may also underlie the sharpening of selectivity for nonspatial features such as color, but, to date, no experimental evidence has been provided. A biologically plausible and explicit implementation of cross-hierarchical selection was developed in the selective tuning (ST) model of visual attention (Tsotsos et al., 1995), which has been generalized to nonspatial selection processes including FBA (Tsotsos, 2011). The ST model posits that attention increases selectivity by a hierarchical winner-take-all process that propagates from higher to lower levels in the visual hierarchy. It thereby eliminates (prunes) the forward contribution of less responsive (nonwinning) units in lower-level layers to the coding of the input. Although this top-down process increases the resolution of target discrimination (Boehler et al., 2009; Hopf et al., 2010), it imposes spatiotemporal constraints on cortical processing (Rothenstein and Tsotsos, 2014); that is, sharpened selectivity will be reached with a temporal delay and this delay will reflect the time required for underlying modulations to propagate from higher to lower levels of cortical representation.

Here, we test these predictions by analyzing the dynamics of attention-driven color tuning in human visual cortex with high spatiotemporal resolution magnetoencephalography (MEG) recordings. To assess tuning, we used a modified version of the unattended probe paradigm used previously (Bartsch et al., 2015). In this paradigm, we record the neuromagnetic response elicited by a spatially unattended color probe in one visual hemifield while subjects discriminate a color-defined target in the other hemifield (cf. Fig. 1*A*). For the present purpose, we gradually changed the degree of color match between the probe and the target. The probe color was varied in seven steps ranging from a full match (prototypical red) toward a prototypical purple, a color that neighbors red in color space. The response variation as a function of probe-to-target color distance served as a measure of population tuning.

Consistent with predictions of the ST model, we find that FBA causes a backward-propagating sequence of modulations in ventral extrastriate cortex. Specifically, color-based attention begins with an initial, coarsely tuned modulation at higher levels of representation. This in turn evolves into a sharper selectivity profile at lower levels facilitated by the attenuation of color values that neighbor the target in color space.

Materials and Methods

Subjects. Thirty-one (19 female, mean age 25.4 years, one left-handed) and 21 (11 female, mean age 27.3 years, one left-handed) subjects participated in the FBA and Control Experiment 1, respectively. Twenty subjects took part in Control Experiment 2 (11 female, mean age 28.0). All subjects gave written informed consent before testing and were paid for participation (6 €/h). All subjects were neurologically normal with normal color vision and normal or corrected-to-normal vision. The experiments were approved by the ethics board of the Otto-von-Guericke University, Magdeburg, Germany.

Stimulus presentation. The stimuli were back-projected by an LCD projector (DLA-G150CLE; Covilex) onto a semitransparent screen (Covilex) placed inside the dimmed, magnetically shielded recording chamber (μ-metal; Vacuumschmelze) at a viewing distance of 1.0 m. Presentation software (Neurobehavioral Systems) was used to coordinate stimulus presentation. Subjects gave responses with a LUMItouch response system (Photon Control).

Stimuli and procedure (FBA experiment). On each trial, a circle (diameter 3.1° of visual angle, center placed 4.9° to the left and 3.1° below fixation) composed of two colored half-circles was presented in the left visual field (LVF) together with a unicolor circle at the mirror image position in the right visual field (RVF) (Fig. 1*A*). One of the two half-circles in the LVF was drawn in a focal red in CIE space (see "Definition of probe colors" section) and the other was assigned randomly one of three other colors (yellow, green, or gray). Colors were psychophysically matched using heterochromatic flicker photometry (Lee et al., 1988). Subjects fixated a permanently visible white central fixation cross on a black background. They attended to the red half-circle (target) in the LVF and reported whether it appeared at the left or right side of the circle with a two alternative button press of the right hand (left: index finger, right: middle finger). The unicolor circle in the RVF (probe) was always task irrelevant and served as a probe to elicit the brain response underlying global color-based attention outside the spatial focus of attention (cf. Bartsch et al., 2015). The color of the probe varied randomly from trial to trial among seven isoluminant color values in the red–purple range span-

ning from the focal target red (R0) to a focal purple (P6) (see "Definition of probe colors" section). As the distance of a color from R0 increased, we used labels with increasing numerical indices, as well as letters indicating subjects' behavioral classification of a given color as red (R1, R2, or R3) or purple (P4, P5, or P6). Subjective color classification was determined in an independent behavioral color categorization test (for details, see below). FBA-mediated color selectivity for the currently attended target color was measured by comparing the brain responses to the different probe colors that varied in color distance to the target. Stimulus frames appeared trial by trial for 300 ms with a varying interstimulus interval of 1000–1200 ms (rectangular distribution). Each subject perfomed 9 trial blocks with each lasting ~5 min and containing 168 trials (every 28 trials, subjects paused for 8 s and were encouraged to blink). This yielded a total of 216 trials for each probe color.

Stimuli and procedure (Control Experiment 1). The stimuli were identical to those of the FBA experiment except for the following modifications as shown in Figure 1*B* (left). First, a rapid serial visual presentation (RSVP) stream was added directly above fixation (the fixation cross was replaced by a small fixation dot. Second, the interstimulus interval between circle presentations was 1230–1430 ms. Third, only five colors of the red–purple range were presented on the probe side (R0, R2, P4, P5, and P6). The RSVP stream consisted of a rapid sequence of 11 white letters randomly selected from a list of 10 uppercase characters (A, E, I, K, L, N, O, T, V, and Y; height: 0.5° visual angle, 32 ms character duration, 48 ms interstimulus interval). The RSVP stream started 290 ms before circle onset and ended 290 ms after circle offset with the presentation of a question mark (650–850 ms). The subjects were to ignore the circles, attend the RSVP stream, and report whether it contained the character "O" with a button press of the right hand (yes: index finger, no: middle finger). The character "O" was present in 50% of the trials.

Each subject performed 3 trial blocks with each lasting ~5 min and containing 150 trials (every 30 trials, subjects were given a 6.5 s pause during which they were encouraged to blink). This yielded a total of 90 trials for each probe color.

Stimuli and procedure (Control Experiment 2). The stimulation protocol was similar to Control Experiment 1 except that a small black bar (height: 1.16°, width: 0.34°) was superimposed onto the double-color circle in the left VF and there was no RSVP stream at fixation (Fig. 1*B*, right). The black bar was tilted randomly to the left or right from the vertical by 30°. Subjects were instructed to fixate the center and discriminate the tilt of the bar while simultaneously ignoring the colored circles. Stimulus frames were again shown for 300 ms and interstimulus intervals varied between 1000 and 1200 ms. Each subject performed six trial blocks, which yielded a total of 144 trials per probe color.

Definition of probe colors. First, a range of isoluminant colors between focal red (R0, the target color) and focal purple (P6) was defined in the following way. The luminance of six colors spanning from focal red to focal purple was psychophysically matched by heterochromatic flicker photometry (Lee et al., 1988). A cubic polynomial was then fitted to these sampling points (MATLAB; The MathWorks, RRID:SCR_001622) to define 49 isoluminant color values (color steps) lying in between focal red (R0) and focal purple (P6). The luminance for all colors in the red–purple range was ~16 cd/m^2. R0 (RGB: 130 0 0, CIE XYZ: 0.6400 0.3300 0.0300) and P6 (RGB: 110 0 110, CIE XYZ: 0.3209 0.1542 0.5249) were kept constant for all observers. To determine subject-specific color values in between, subjects first underwent a staircasing procedure to derive the individual discrimination threshold (R2) for the target red (R0). To this end, subjects were presented two unicolored circles of a size and position matching that of the target and probe in the FBA experiment. The left circle (target position) was always drawn in focal red (R0), whereas there was a 50% chance that the right circle (probe position) would be assigned a color different from R0 of the red–purple range, starting with focal purple and becoming progressively more red during the staircase procedure. Subjects had to attend to both color circles and indicate with a two-alternative choice response whether the colors were equal (index finger) or not (middle finger). The staircase followed a one-up/one-down procedure with eight reversals (first and second reversal discarded, values of last six reversals averaged). The step size started with two color steps at a time and was decreased to one color steps after the second reversal. Each subject repeated the staircase procedure until three stable values were attained. R2 was then calculated by averaging the results of those three staircases (average R2 coordinates: RGB: 130 0 27, CIE XYZ: 0.5031 0.2546 0.2423).

Two reds were then chosen 2 SDs below (R1) and above (R3) the discrimination threshold R2, but always with a minimum distance to the threshold of three color steps. That way, R1 (average coordinates: RGB: 131 0 21, CIE XYZ: 0.5272 0.2678 0.2050) and R3 (average coordinates: RGB: 130 0 33, CIE XYZ: 0.4825 0.2432 0.2743) were always three or four color steps away from R2 for all the subjects. Finally, the color space from R3 to P6 was divided in three equidistant steps, placing the remaining purple values P4 (average coordinates: RGB: 126 0 54, CIE XYZ: 0.4222 0.2100 0.3678) and P5 (average coordinates: RGB: 118 0 79, CIE XYZ: 0.3678 0.1800 0.4522). Therefore, the color range from R0 to P6 included five approximately equidistant steps (R0, R1, R3, P4, P5, and P6). Color distances between R1 and R2 and R2 and R3 were smaller to allow to assess brain activity around the discrimination threshold. Importantly, whereas there was some individual variance concerning the discrimination threshold R2 (SD = 1.85 color steps), P4 and P5 were less variable across subjects (both SDs $\leq$ 1.24 color steps). The seven probe colors individually determined for each subject before the FBA experiment were also used for the behavioral color categorization test that was performed in a subset of these subjects (see "Color categorization test" section). In both control experiments, five colors of the FBA experiment were presented (R0, R2, P4, P5, and P6; average coordinates).

Color categorization test. Twenty-four subjects who participated in the FBA experiment took also part in a behavioral color categorization test (mean age 26.9 years, 15 female, one left-handed). The test was conducted to determine where subjects would place the categorical border between red and purple relative to the range of probe colors used in the FBA experiment. Every subject participated in two versions of the test: one with the seven probe colors as used in the FBA experiment (R0, R1, R2, R3, P4, P5, and P6) and one with 11 probe colors dividing the red–purple range (51 colors spanning from R0 to P6, as defined above) into 10 equidistant steps. Both versions were run in the same test session, starting with the seven colors. Stimulus timing and stimulus geometry are shown in Figure 1*C*. Subjects' fixation remained on the central fixation cross while they were covertly attending the probe location in the RVF where a unicolor circle (probe) was presented on each trial as in the FBA experiment. No stimulus appeared in the LVF. The probe color varied randomly from trial to trial between either the seven or the 11 color values. Subjects were asked to report whether the probe's color was a red or a purple with a two alternative button press of the right hand (index vs middle finger). Color-to-finger assignment was counterbalanced across subjects. To provide consistent color reference over trials, circles drawn in R0 and P6 were presented for 667 ms before the probe (1100 ms SOA, probe presentation duration: 300 ms). Assignment of R0 and P6 to reference circle positions changed blockwise. Trials were terminated by response button press or ended otherwise automatically 3700 ms after probe offset (after 3200 ms, a "timeout" sign was presented for 500 ms). The next trial always started with a 450 ms delay. The centers of the reference color circles R0 and P6 (diameter 3.1° visual angle) were positioned 1.3° below and 5.6° right from fixation cross (upper circle) and 4.7° below and 3.5° right from the fixation cross (lower circle). Subjects performed four blocks of the seven-color-metric (each with 147 trials) and subsequently six blocks of the equidistant 11-color-metric (each with 154 trials). Each block lasted on average ~6 min. Every 30–31 trials, the participants were given a 7 s pause during which they were encouraged to blink. All in all, this yielded 84 trials for each color for both the seven and the 11 color metric. Behavioral results are shown in Figure 1*D*.

MEG recordings. The MEG was recorded continuously with a 248 sensor BTI-Magnes 3600 magnetometer system (4D Neuroimaging). Vertical and horizontal eye movements were monitored simultaneously (Synamps amplifier; Neuroscan) by recording the electro-oculogram (EOG) from bipolar electrode placements at the outer canthi of both eyes (horizontal EOG) as well as from a unipolar placement below the right eye (vertical EOG). MEG and EOG were low-pass filtered (DC to 50 Hz) in the analog domain and then digitized with a sampling frequency of 254.31 Hz. For primary data analysis, the continuous MEG and EOG data

were epoched offline into time windows extending from 200 ms before to 700 ms after stimulus onset (stimulus-locked event-related responses). Artifact rejection was performed by excluding epochs in which peak-to-peak amplitude differences exceeded an individually defined threshold. The latter was adjusted iteratively in each subject until the data were devoid of major artifacts, resulting in 1–16% percent of rejected trials (mean: 7%). Applied thresholds ranged between 1.8 and 3.6×10^{-12} T for the MEG (mean: 2.6 pT) and 60–165 μV for the EOG (mean: 91 μV).

MEG data analysis. The event-related magnetic response was averaged selectively for each probe color and subject (computed relative to a 200 ms baseline). Data were then averaged over subjects to derive probe-color-specific grand average responses. Because head positons could vary relative to the MEG sensory array, individual datasets were aligned before averaging data across subjects (see "Coregistration of anatomical data and sensor positions" section). Current source density (CSD) analysis was performed using minimum norm least-squares (MNLS) estimates as implemented in Curry 7 (Neuroimaging Suite, Compumedics; Neuroscan, RRID:SCR_009546; Fuchs et al., 1999). Estimates were constrained by a realistic average head model (standard brain) provided in Curry 7.

Coregistration of anatomical data and sensor positions. For coregistration of the MEG with anatomical data, individual landmarks (nasion, left and right preauricular point) as well as five localizer coils placed at standardized positions over the skull were digitized using the 3Space Fastrak System (Polhemus). For grand average data analysis, sensor position data of each individual subject were brought into reference with a canonical sensor array using the lead-field inversion approach. Specifically, the measured data were repositioned to reference sensor locations that represent the most canonical position of sensors relative to anatomical landmarks (selected from 1500 recording sessions done in our MEG laboratory). For repositioning, we computed for each subject the individual lead-field matrix with Curry 7 using the MNI brain (Montreal Neurological Institute, ICBM-152 template) as source space and volume conductor model. Those lead-fields were (pseudo-)inverted (MNLS approach) to transform the individual data from sensor space in MNI source space and then back-projected into the reference sensor space. The latter was done by a forward projection using the lead-field belonging to the reference sensor locations. This way, subject-specific data were recomputed as if they all would have been recorded with the same (reference) head position with respect to the MEG sensor array.

Experimental design and statistical analysis. Statistical validation of the probe-color-dependent response variation was performed at sensor level in several steps. First, to determine the time range of significant overall response variation, we used a time sample by time sample sliding window (30 ms) statistical testing (repeated-measures ANOVA (rANOVA), seven-level factor probe color for FBA experiment, five-level factor probe color for control experiments) in a time range between 0 and 500 ms after stimulus onset relative to baseline. The first of five or more consecutive time samples with $p \leq 0.05$ was considered as effect onset (for a conceptual background, see Guthrie and Buchwald, 1991). Second, the probe-color-dependent response variation was tested in selected time windows after probe onset by computing rANOVAs on average response amplitudes in those time windows. To characterize the relative change of reponse amplitudes between individual probe colors, selected *post hoc* paired comparisons (dependent t tests) were computed. The resulting increase of the type I error was controlled for by correcting the nominal α level ($p = 0.05$) following the approach of Cross and Chaffin (1982). The corrected level is indicated at relevant places in the Results section. Violations of sphericity were corrected using the Greenhouse–Geisser ε (corrected p-values are reported). Third, statistical validation of between experiment variation (FBA experiment vs Control Experiments 1 and 2) was performed on the response amplitudes in time windows of interest using a mixed-design ANOVA with the between-subjects factor experiment and the within-subjects factors probe color (five levels) and time window (three levels). The bar plots and all statistical validation were based on unfiltered data. For visualization purposes, a smoothing Gaussian filter (time domain SD of four sample points) was applied to the waveforms shown in Figures 3, 5, and 6.

Clustering validity analysis and probabilistic maps (FBA experiment). For this analysis, all data were transformed into source space using MNLS estimates as implemented in Curry 7 (Fuchs et al., 1999). Estimates were constrained by a realistic average head model (standard brain) provided in Curry 7. The resulting source space representation of each probe color was then subjected to a topographical clustering validity analysis (see below), yielding a cortical map of clustering validity parameters (silhouettes; Rousseeuw, 1987). Those silhouette maps were finally coregistered with probabilistic maps of hV4, VO-1, and area PHC-2 (Wang et al., 2015). Surface segmentation, triangularization, and coregistration of the atlas data were performed using routines available in FreeSurfer version 5.1.) and FSL (http://www.fmrib.ox.ac.uk/fsl/, RRID:SCR_001847).

Clustering validity analysis. The binary clustering validity analyses were performed to determine the cortical locus of coarse and sharpened selectivity for the attended color (R0). The general logic behind this approach is to find the cortex location showing largest clustering validity (maximal silhouette coefficients, see below) when the seven probe colors are assigned to two clusters with fixed membership in which P4 is either in one cluster together with the other reds (coarse selectivity) or in one cluster together with the other purples (sharpened selectivity). Silhouette coefficient as a measure of clustering validity: The silhouette value $s(i)$ of a data point i is a measure of its similarity to its containing cluster relative to its similarity to the neighboring cluster (Rousseeuw, 1987), where $-1 \leq s(i) \leq 1$. A silhouette value <0 indicates that i is closer to the members of the neighboring cluster than to the members of its containing cluster; a value near 0 indicates that i lies between two clusters; and a value near 1 indicates that i has been assigned appropriately to its cluster. The silhouette coefficient of a dataset is the arithmetic average of all silhouette values, thus indicating how well the data have been clustered overall (clustering validity).

Probabilistic maps: fMRI recordings and retinotopic mapping. To determine probabilistic maps of area hV4 and VO-1, retinotopic mapping was performed in eight subjects using a standard stimulation protocol (moving bars) specifically designed to measure population receptive fields (Dumoulin and Wandell, 2008; Amano et al., 2009).

Functional images were acquired with a 3 T Siemens Prisma scanner (TE = 30 ms, TR = 2 s, 90° flip angle, 128 × 128 FoV). In each of six runs, 15 consecutive bar sweeps (duration 28 s) were presented in steps of 24° resulting in 220 scans per run, including 10 scans to account for hemodynamic decay. The moving bar stimulus progressed across a gray circular region subtending a 400 px radius. The bar was created by revealing a flickering checkerboard background (8 Hz). The width of the bar was 20 px. To ensure proper fixation throughout the session, subjects had to report sudden color changes of the fixation dot occurring randomly every 4–7 s. Functional images consisting of 28 slices with a resolution of 2.0 × 2.0 × 2.0 mm were recorded perpendicular to the calcarine fissure covering the occipital lobe.

Functional images were resliced, registered to the first image of the session, and smoothed with a 2 mm kernel. Two-dimensional spatial population receptive field (pRF) profiles for each voxel were estimated by back-projecting the detrended and deconvolved 1-D fMRI time series for each sweep angle (Lee et al., 2013; Greene et al., 2014). Angular position and eccentricity of each receptive field was derived from the maximum of its pRF profile.

For each subject performing the retinotopic mapping, a structural image was acquired (1.0 × 1.0 × 1.0 mm, TR = 2500 ms, TE = 4.77 ms, TI = 1100 ms, 7° flip angle, 256 × 256 FoV) to create high-resolution surface reconstructions of the cortex using FreeSurfer (https://surfer.nmr.mgh.harvard.edu, RRID:SCR_001847). Polar and eccentricity maps were subsequently registered to the structural image and mapped onto the final reconstruction of the cortical surface. Within this surface space, early visual areas were identified manually for each subject using the individual angular and eccentricity maps. Using surface normalization, each labeled region of each subject was projected onto the standard FreeSurfer surface (fsaverage). Subsequently, the same labels for each region were averaged across all eight subjects to establish probability maps of early visual areas in standard FreeSurfer surface space. To localize these areas within the standard Curry surface, the Curry surface was converted into FreeSurfer space and a projection onto the standard FreeSurfer surface was established. Probability maps of visual areas shown in Figure 4 were subsequently projected onto the standard curry surface.

The coverage of the retinotopic scans did not reach areas such as PHC-2, which are situated anterior to the map of VO-1/2 (Arcaro et al., 2009). The map of PHC-2 in Figure 4 therefore shows the distribution of this area as defined in the probabilistic atlas of topographically defined visual areas (www.princeton.edu/~napl/vtpm.htm) (Wang et al., 2015). The atlas data were converted into FreeSurfer space and then projected onto the standard Curry surface.

Results

Experiment 1: FBA experiment

Subjects response accuracy was high on the "left/right" color discrimination task (on average 96% correct responses with a reaction time of ~414 ms), confirming that they were consistently attending to the target color. Analogously to the data analysis in Bartsch et al. (2015), brain activity reflecting FBA to the target color was derived by subtracting the response elicited by the probe with the largest color distance from the response to each other probe color (R0 − P6, R1 − P6, R2 − P6, R3 − P6, P4 − P6, and P5 − P6). Because the stimulation on the target side is the same for all probe colors, this subtraction eliminates all target-related response variation but leaves the response variation (relative to P6) due to probe color distance.

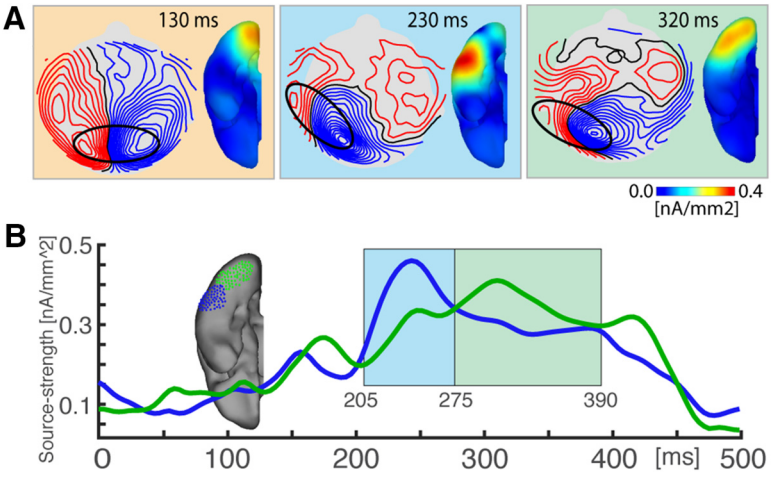

Figure 2. Magnetic field maps and source localization results of the FBA experiment (overall response). ***A***, Field maps and corresponding current source density distributions of the average FBA response at three selected time points (130 ms, orange; 230 ms, blue; and 320 ms, green) after probe onset. The black ellipses highlight the magnetic field components (efflux–influx configurations, red– blue) that give rise to the current source maxima visible in the 3D CSD maps. ***B***, Time course of average CSD estimates in ROIs (blue/green dots in the 3D map) corresponding with the anterior (blue) and posterior ventral extrastriate maximum (green) of the FBA response. The colored windows mark the early and late time ranges that served to analyze the FBA response in ventral extrastriate cortex as a function of probe color distance. Blue marks the time range (205–275 ms) during which source activity in the anterior ROI reached the temporal maximum and was stronger than in the posterior ROI. Green highlights the time range (275–390 ms) during which source activity in the posterior ROI showed a temporal maximum and was stronger than the anterior ROI.

FBA modulations (overall response)

Figure 2*A* plots the magnetic field distribution and corresponding source localization (CSD maps) of the overall response difference (average over all six probe color differences) at three representative time points after stimulus onset. The time points are chosen to best illustrate the spatiotemporal change of the magnetic field distribution as it evolves in visual cortex contralateral to the probe. The magnetic response shows a first peak (130 ms, highlighted in orange) in early visual cortex (consistent with V1), followed by a maximum at 230 ms in ventral extrastriate cortex (highlighted in blue). The extrastriate response, initially peaking in more anterior regions, then transitions to more posterior ventral regions to reach a maximum at ~320 ms (highlighted in green). This posterior propagation of the extrastriate activity maximum over time is further illustrated in Figure 2*B*, which shows the time course of average CSD in regions of interest (ROIs) defined by the source activity maxima at 230 (blue dots) and 320 ms (green dots). The more anterior ROI shows a steep rise of source activity starting at ~200 ms, which exceeds the response of the posterior ROI between 205 and 275 ms (blue window). The more posterior ROI shows a delayed activity increase with a maximum at 320 ms and exceeds the response of the anterior ROI between 275 and 390 ms (green window). The time windows highlighted in blue and green in Figure 2*B* will serve to define the time ranges in which the ventral extrastriate magnetic field responses will be analyzed in more detail as a function of probe color distance.

FBA modulations as a function of probe color distance

Figure 3 shows the response separately for each of the six probe color differences at selected sensor sites best representing the early visual (Fig. 3*A*), the initial anterior extrastriate (Fig. 3*B*), and the later more posterior extrastriate modulations (Fig. 3*C*). Time ranges of significant overall differences (sliding one-way seven-level rANOVA) are indicated by black horizontal bars under the waveforms. The bar plots on the right show response averages in time windows of interest highlighted by the color squares of the initial early visual cortex response (110–150 ms, orange), as well as the early (205–275 ms, blue) and late (275–390 ms, green) extrastriate responses. One-way rANOVAs with the seven-level factor probe color confirmed that the response variation was highly significant in all selected time ranges (110–150 ms: $F_{(6,180)} = 6.89, p < 0.0001$); 205–275 ms: $F_{(6,180)} = 20.27, p < 0.0001$; 275–390 ms: $F_{(6,180)} = 12.25, p < 0.0001$).

As visible in Figure 3*A*, the response in early visual cortex shows a gradual decrease with increasing distance to the target color. During the subsequent response maximum in anterior ventral extrastriate cortex (Fig. 3*B*), all reds (R0–R3) show a large amplitude, whereas the amplitude of P5 is small and similar to that of P6. Window averages on the right (blue bar plot in Fig. 3*B*) show that the P4 response exhibits a large amplitude more similar to the red responses, as opposed to the purple responses. That is, the response enhancement encompasses purple values close to red, indicative of a rather coarse selectivity for the target red. Paired comparisons (dependent *t* tests) on mean amplitudes between 205 and 275 ms confirm that all reds, as well as P4, differ from P5 and P6 (all $p \leq 0.00007$, corrected α-level $p = 0.025$), whereas there was no significant difference between P5 and P6 ($p = 0.13$). After 275 ms, the modulation profile changes qualitatively in that the P4 response is attenuated to the level of P5. This change is prominent at the sensor representing the posterior ventral extrastriate maximum (Fig. 3*C*). The window averages between 275 and 390 ms (green bar plot in Fig. 3*C*) display a marked amplitude fall-off between R3 and P4, which indicates a sharpened selectivity profile compared with the earlier (205–275 ms) time range. Paired comparisons confirm this change in profile. All purples, including P4, are significantly different from the reds (all $p \leq 0.0101$) except for the R1 versus P4 comparison, which approached significance ($p = 0.018$) at the corrected

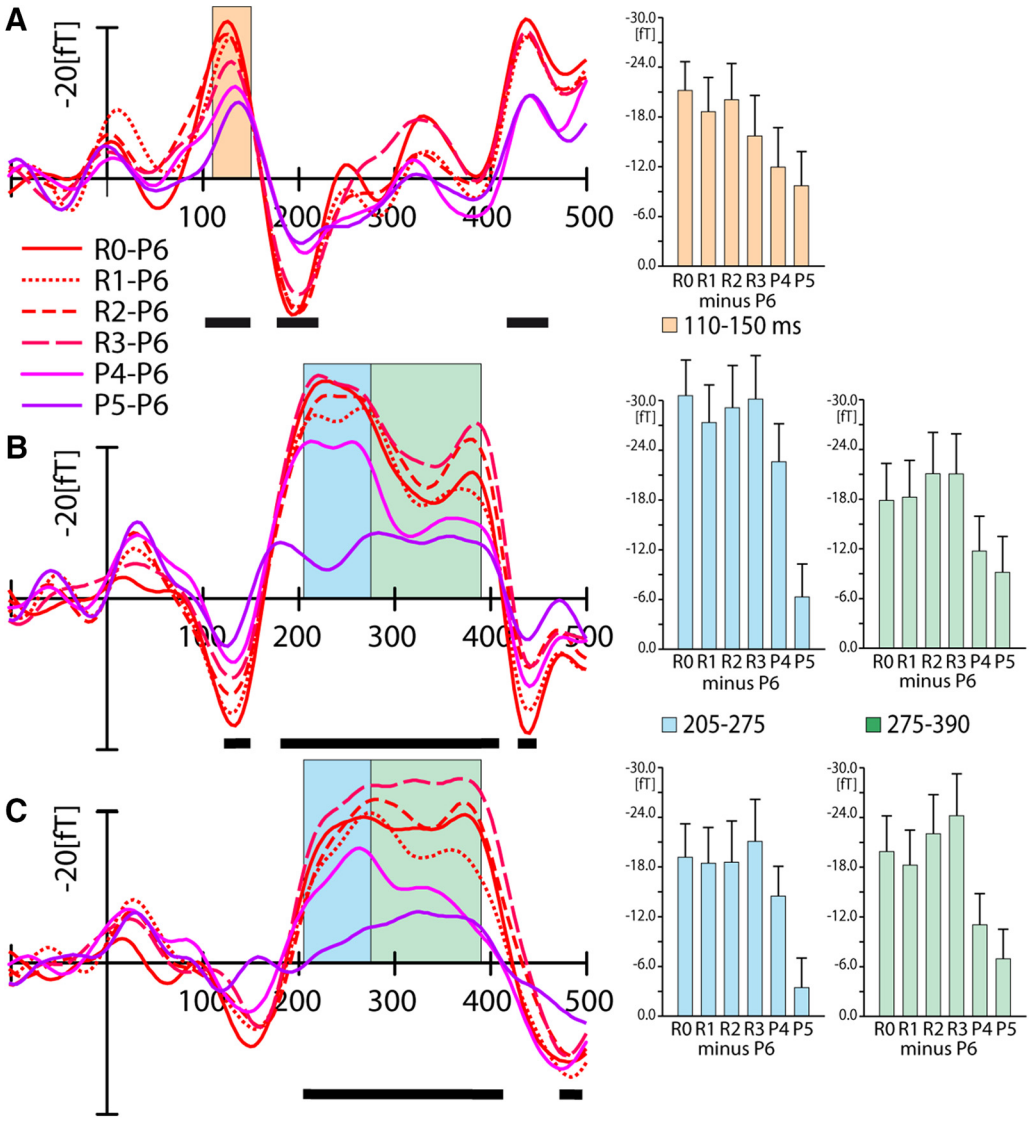

Figure 3. Magnetic response as a function of probe color distance (FBA experiment). ***A–C***, Difference waveforms (probe color minus P6 difference) at selected sensor sites representing the initial response in early visual cortex (***A***) and the subsequent response in anterior (***B***) and in posterior ventral extrastriate cortex (***C***) . Black horizontal bars index the time range of significant overall response differences between probe colors (time-sliding one-way seven-level rANOVA; see Materials and Methods). The colored windows highlight the time range in which response averages, shown in the bar plots on the right, were computed. Window averages of the 110–150 ms, 205–275 ms, and 275–390 ms range are plotted in orange, blue, and green, respectively. Error bars indicate SEM.

α-level ($p = 0.0125$). Relative to R0, the R1 and R3 responses show decreased and increased amplitudes, respectively. Paired comparisons, however, reveal that the amplitude difference between R1 and R3 did not reach significance ($p = 0.063$) and neither R3 ($p = 0.13$) nor R1 ($p = 0.51$) differed significantly from R0.

It should be noted that the sharpening of the response profile associated with an anterior-to-posterior propagation is most prominent when comparing the early response window of the anterior sensor site (blue in Fig. 3*B*) with the later window of the posterior sensor site (green in Fig. 3*C*). Nonetheless, the sharpening over time is also visible, although to a lesser degree, at each sensor site alone. This is because the field distributions corresponding with the anterior and posterior ventral extrastriate CSD maximum between 200 and 400 ms are not very different (compare the field distributions in Fig. 2*A*, blue and green). The sensors, selected to best represent the anterior and posterior extrastriate modulation, will therefore show field overlap reflecting both current maxima, with the anterior–posterior propagation of coarse-to-sharpened selectivity appearing as a relative effect in the overlapping field response.

Finally, it is worth annotating that the sharp fall-off between R3 and P4 coincides with the subjective categorical border between red and purple (Fig. 1*D*).

Cluster validation of selectivity changes

The source localization analysis of the overall magnetic field response (Fig. 2) revealed that the FBA-related modulation in extrastriate cortex propagates in reverse hierarchical direction from more anterior to more posterior regions. The detailed analysis of the magnetic field response to the probe as a function of color distance to the target suggested that this posterior propagation is associated with an increase of color selectivity over time that is particularly prominent at lower hierarchical levels. To further validate that color selectivity increases in reverse hierarchical direction, we transformed the magnetic field response to each probe color into source space and subjected the data to a binary

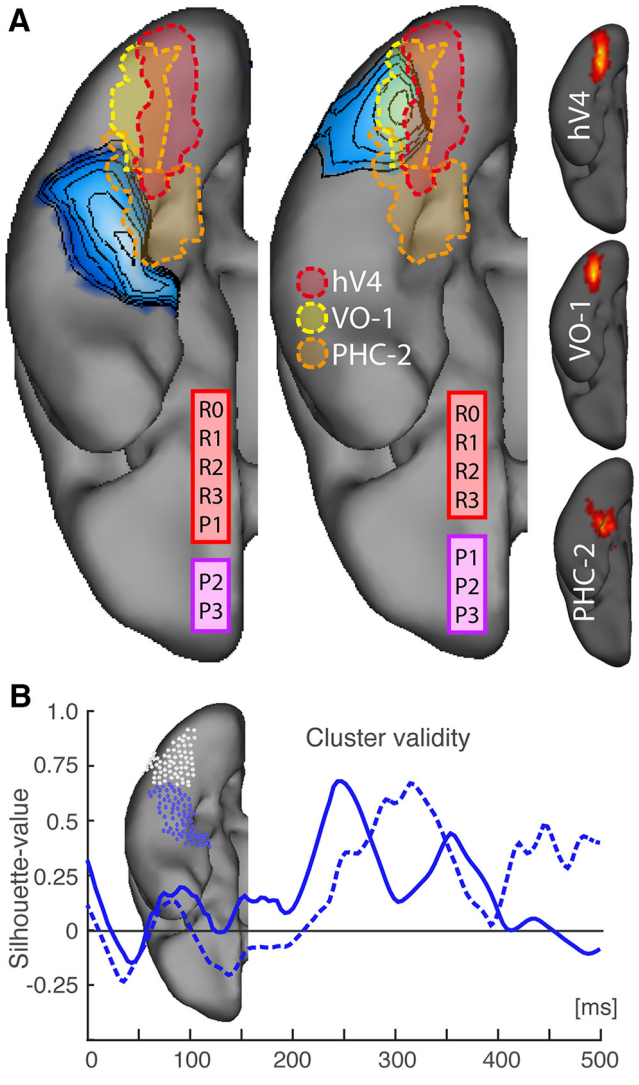

Figure 4. Cluster validity analysis (FBA experiment). ***A***, 3D maps showing maxima of cluster validity (silhouette values, blue) for a given membership assignment testing coarse selectivity for R0 ([R0,R1,R2,R3,P4] [P5,P6], left) versus sharpened selectivity for R0 ([R0,R1,R2,R3,] [P4,P5,P6], right). The overlaid dashed outlines mark the extension of areas hV4 (red), VO-1 (yellow), and PHC-2 (orange). The outlines highlight probabilistic distributions (shown on the far right) derived from a subset of eight subjects participating in the reported experiments (hV4, VO-1) or from the probabilistic atlas of topographically defined visual areas (PHC-2) (Wang et al., 2015). ***B***, Time course of the average cluster validity in ROIs defined by the anterior (blue dots, solid blue trace) and posterior (white dots, dashed blue trace) silhouette maximum shown in ***A***.

(red vs non-red) fuzzy-clustering validity analysis (see Materials and Methods) at each location of the source space (3D-rendered gray matter surface of the MNI152 brain). Coarse selectivity for R0 was tested using two clusters, one containing all reds plus P4 and the other containing P5 and P6. Sharpened selectivity was tested with one cluster containing all reds and the other containing all purples. Figure 4*A* shows silhouette maps (blue) highlighting cortical regions where source activity variation yields the highest clustering validity. Thresholds for the coarse (left) and sharpened selectivity map (right) are demarcated in accordance with the maximum. Superimposed are probabilistic maps of retinotopic area hV4 (red), ventral occipital area VO-1 (yellow), and parahippocampal area PHC-2 (orange). As can be seen, the silhouette maximum of sharpened selectivity coincides with posterior ventral retinotopic area VO-1 and partially overlaps with area hV4. In contrast, the maximum of coarse selectivity is localized to the anterior ventral extrastriate cortex beyond hV4 and VO-1, in a region lateral to (and partially overlapping with) PHC-2. Apparently, the silhouette maximum of coarse selectivity arises in a nonretinotopic area that is higher in the ventral extrastriate processing hierarchy than VO-1 and hV4. Figure 4*B* shows the time course of average silhouette values in ROIs defined by the coarse (Fig. 4*B*, blue dots) and sharpened (Fig. 4*B*, white dots) selectivity maxima visible in Figure 4*A*. Coarse selectivity in anterior ventral extrastriate cortex (Fig. 4*B*, solid blue) increases at 200 ms to reach a maximum at ~240 ms. Sharpened selectivity in more posterior VO-1/hV4 (Fig. 4*B*, dashed blue), in contrast, rises with a delay and reaches its maximum at ~320 ms. Therefore, the results of the cluster validity analysis confirm that the sharpening of population tuning appears with a delay and in hierarchically lower extrastriate areas than the prior coarsely tuned response modulation.

Control experiments: Control Experiment 1

In the FBA experiment, the selectivity for the target color was assessed by comparing the magnetic response to probe colors with increasing distance to the target in color space. One potential issue with this way of testing selectivity is the inevitability of comparing physically different probe colors. Although matched in luminance, low-level sensory differences could potentially cause some of the response differences attributed to FBA. To address this possibility, we ran a control experiment in which the target and the probe were presented as in the previous FBA experiment, but with attention being directed away from those items. This was accomplished using an RSVP discrimination task at fixation (Fig. 1*B*, left). Only five probe colors were used in this experiment (R0, R2, P4, P5, and P6). Otherwise, the data analysis was performed as in the FBA experiment. RSVP performance was high (on average 95.5% hits, 427.7 ms reaction time), verifying that subjects were consistently attending to the RSVP stream and ignoring the peripheral stimuli. The magnetic data of Control Experiment 1 are shown in Figure 5. As in the FBA experiment, the overall response difference against P6 shows an initial CSD maximum in early visual cortex at ~150 ms (Fig. 5*A*, orange). A one-way 5-level rANOVA revealed a significant probe-color-dependent response variations in the 110–150 ms window ($F_{(4,80)} = 4.96$, $p = 0.0038$). Corresponding waveforms and window averages (110–150 ms) computed for the different probe color distances are displayed in (Fig. 5*B*), which reveal a graded response enhancement with increasing similarity to the target color. The profile is qualitatively similar to the one seen in the FBA experiment (replotted as orange circles in the bar plot on the right of Fig. 5*B*), suggesting that the initial response variation, indeed, reflects some low-level sensory difference between probe colors. In the following time range (205–275 ms), the overall response difference shows only minimal source activity in anterior extrastriate cortex (Fig. 5*A*, blue). Corresponding waveforms and window averages are displayed in Figure 5*C*. Compared with the FBA experiment (Fig. 5*C*, blue circles), the probe-related response variation between 205 and 275 ms (Fig. 5*C*, blue) is only small and not significant ($F_{(4,80)} = 1.61, p = 0.196$), consistent with the interpretation that FBA increases the gain of the attended color values, although with low selectivity (i.e., strong enhancement for all reds and P4) in this time range. Finally, in the late time range (275–390 ms), there is no visible source activity in ventral extrastriate cortex (Fig. 5*A*, green). The color-dependent-response variation on the sensors fails to reach significance ($F_{(4,80)} = 2.28$, $p = 0.089$). Corresponding window averages of the response at

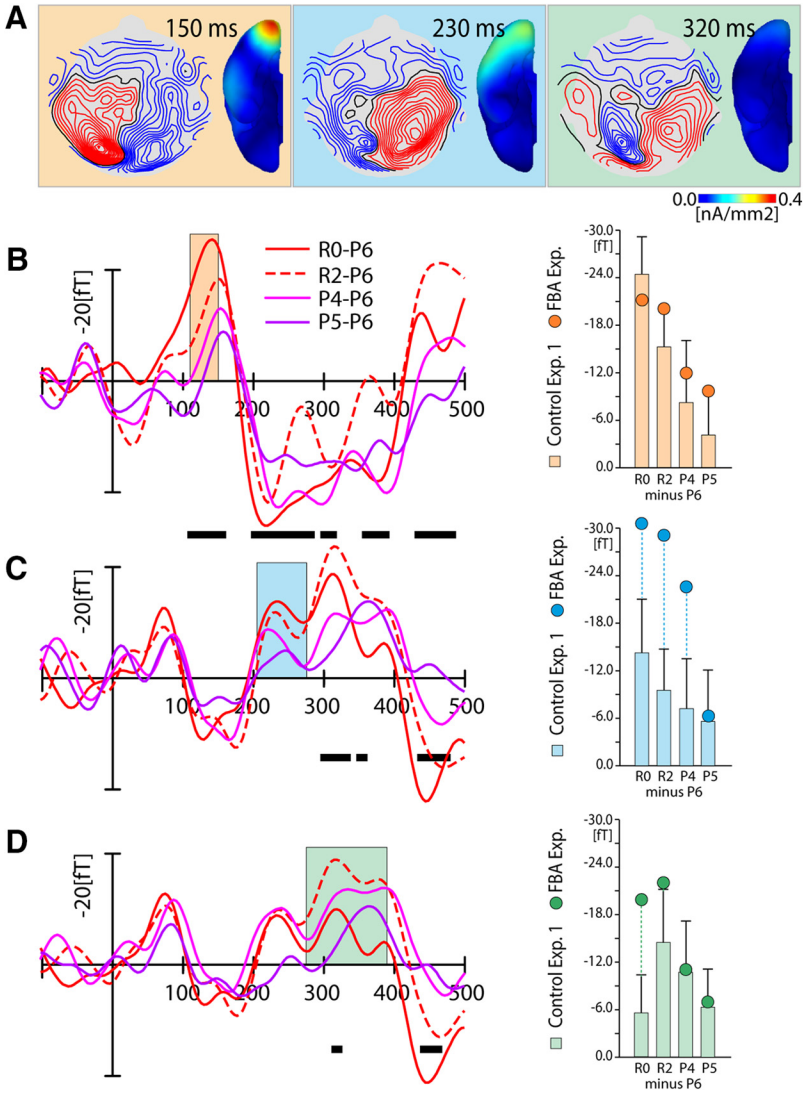

Figure 5. Results of Control Experiment 1. ***A***, Magnetic field maps and corresponding current source density distributions of the average probe response at 150 ms (orange), 230 ms (blue), and 320 ms (green) after probe onset. ***B–D***, Magnetic difference waveforms (probe color minus P6 difference) for each probe color distance at selected sensor sites corresponding with the response in early visual cortex (***B***) and in anterior (***C***) and posterior (***D***) ventral extrastriate cortex. Black horizontal bars index the time range of significant response differences (time-sliding one-way five-level ANOVA; see Materials and Methods). The colored windows highlight the time ranges (defined in the FBA experiment) for which response averages are plotted on the right. Orange, blue, and green bar plots show window averages in the 110–150 ms, 205–275 ms, and 275–390 ms time range, respectively. The colored circles replot window averages of the FBA experiment (Fig. 3) for comparison. Error bars indicate SEM.

the sensor site representing the posterior extrastriate maximum in the FBA experiment in this time range (Fig. 5*D*, green) show no strong amplitude fall-off between reds and purples, which indicated sharpened tuning in the FBA experiment (Fig. 5*D*, green circles).

To validate the differences over time between the response profiles of the FBA experiment and the Control Experiment 1, we computed a three-way ANOVA using a mixed design with the within-subjects factors probe color (R0, R2, P4, P5, and P6) and time window (110–150 ms, 205–275 ms, and 275–390 ms) and the between-subjects factor experiment (FBA, Control 1). The analysis revealed a significant main effect of probe color ($F_{(4,200)} = 24.85$, $p < 0.0001$) and time window ($F_{(2,100)} = 51.53$, $p < 0.0001$), but no effect of experiment ($F_{(1,50)} = 0.29$, $p = 0.594$). There was a significant two-way interaction between time window and experiment ($F_{(2,100)} = 4.25$, $p = 0.017$), whereas the probe color × experiment interaction ($F_{(4,200)} = 1.89$, $p = 0.113$) and the probe color × time window interaction did not reach significance ($F_{(8,400)} = 1.70$, $p = 0.096$). Importantly, there was a significant three-way interaction among probe color, time window, and experiment ($F_{(8,400)} = 2.26$, $p = 0.023$), confirming that the change of the response profile over time as a function of probe color in the FBA experiment is not present in Control Experiment 1.

In sum, withdrawing attention from the color target preserved the pattern of response variation in early visual cortex, suggesting that the very initial response in V1 reflects sensory differences between probe colors. In contrast, later modulations in extrastriate visual cortex are small and inconsistent, which indicates that the modulations seen in the FBA experiment after ~200 ms truly reflect the operation of FBA.

Control Experiment 2

One may object that, whereas the RSVP task in Control Experiment 1 effectively withdraws attention away from the color circle, it does not properly control for the distribution of spatial attention. In the FBA experiment, the spatial focus was extrafoveal and directed to the color target in the LVF. In Control Experiment 1, the focus was foveal and the color circle appeared outside the spatial focus of attention. Control Experiment 1 therefore does not control for the possibility that the sharpening of the response profile in the FBA experiment is a mere consequence of presenting color in the spatial focus of attention. To rule out this possibility, it would be necessary to keep the spatial focus as in the FBA experiment while simultaneously withdrawing attention from the color circle. In Control Experiment 2, we addressed this issue by superimposing a small black bar onto the color circle in the LVF. The bar was tilted left or right from vertical. Subjects were instructed to ignore the color circle and discriminate the tilt of the bar. Otherwise, the experimental procedure and data analysis were comparable to Control Experiment 1. Performance was high (on average 96.4% hits, and 450.3 ms reaction time). Figure 6*A* shows field distributions and CSD maps of the overall response difference against P6 at selected time points after stimulus onset corresponding to the maxima of the FBA experiment. As in the FBA and the Control Experiment 1, there is a prominent initial maximum in early visual cortex peaking around 130 ms (Fig. 6*A*, orange). At subsequent time points in ventral extrastriate cortex, however, there is very little (230 ms) or no discernible source activity (320 ms). One-way 5-level rANOVAs revealed significant probe-color-dependent response variations in the initial 110–150 ms window ($F_{(4,76)} = 9.06$, $p = 0.00013$), but not in later time ranges (205–275 ms: $F_{(4,76)} = 1.31$, $p = 0.275$; 275–390 ms: $F_{(4,76)} = 1.47$, $p = 0.233$). As visible in Figure 6*B*, the early visual

cortex response shows a significant gradual reduction with color distance to R0, again emphasizing that the initial response variation reflects low-level sensory differences between probe colors. In the following time range (205–275 ms), the average response difference shows very little source activity in extrastriate cortex (Fig. 6*A*, blue). The corresponding response amplitude variation as a function of probe color displayed in Figure 6*C* is small and not significant, again suggesting that FBA increases the gain of the attended color values in this time range (cf. blue circles in Fig. 6*C* replotting the response amplitudes of the FBA experiment). In the later 275–390 ms time range, there is no discernable source activity in ventral extrastriate cortex (Fig. 6*A*, green). Corresponding magnetic waveforms and window averages for the different probe colors shown in Figure 6*D* show a small and nonsignificant amplitude variation without any indication of a sharpening of the response profile between reds and purples as seen in the FBA experiment (replotted as green circles).

To verify the difference of the response profiles between the Control Experiment 2 and the FBA experiment, we computed a mixed-design ANOVA with the within-subjects factors probe color (R0, R2, P4, P5, and P6) and time window (110–150 ms, 205–275 ms, and 275–390 ms) and a between-subjects factor experiment (FBA, Control 2). The analysis yielded significant main effects of probe color ($F_{(4,196)} = 25.07$, $p < 0.0001$), time window ($F_{(2,98)} = 26.51$, $p < 0.0001$), and experiment ($F_{(1,49)} = 4.50$, $p = 0.039$). There was a significant two-way interaction between probe color and experiment ($F_{(4,196)} = 3.97$, $p = 0.004$), but no significant interaction between time window and experiment ($F_{(2,98)} = 1.35$, $p = 0.265$) or between probe color and time window ($F_{(8,392)} = 1.73$, $p = 0.091$). Again, a significant three-way interaction among probe color, time window, and experiment ($F_{(8,392)} = 4.48$, $p < 0.0001$) was yielded, confirming that the change of the probe-related response profile over time seen in the FBA experiment is not present in the Control Experiment 2.

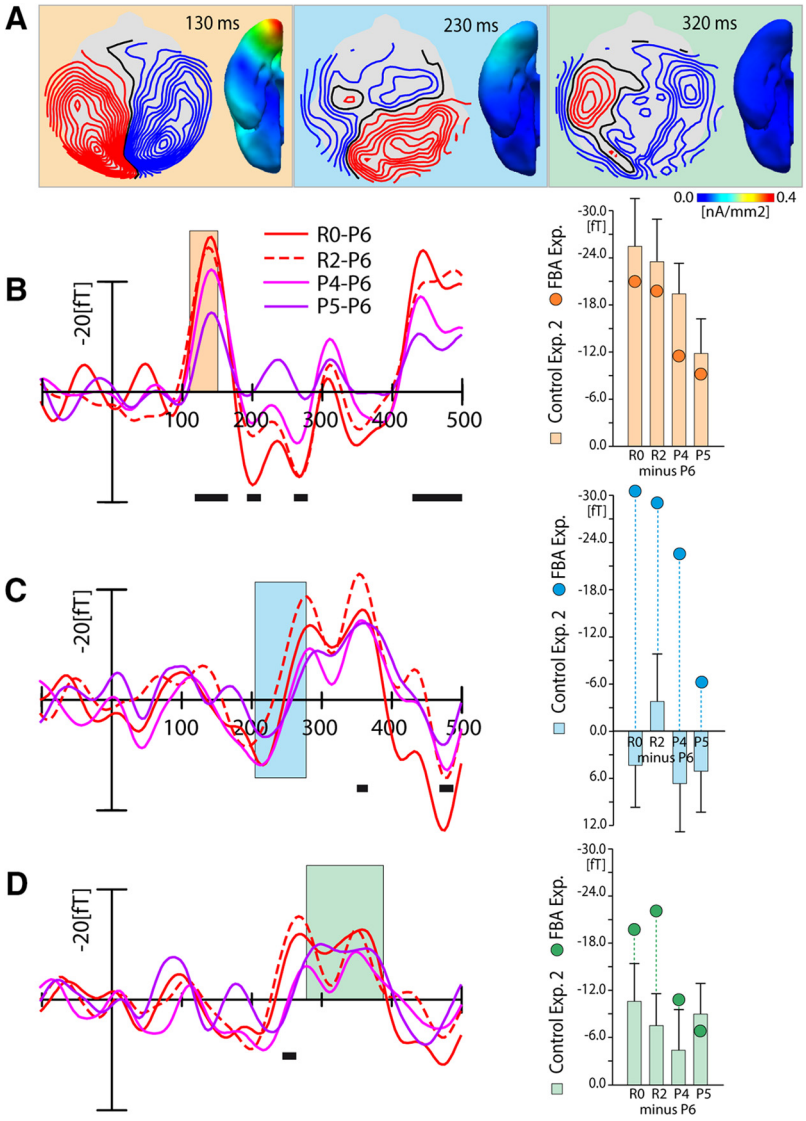

Figure 6. Results of Control Experiment 2. ***A***, Magnetic field maps and CSD distributions of the average probe response at 130 ms (orange), 230 ms (blue), and 320 ms (green) after probe onset. ***B–D***, Difference waveforms (probe color minus P6) for each probe color distance at selected sensor sites corresponding with the response in early visual cortex (***B***), in anterior (***C***) and posterior (***D***) ventral extrastriate cortex. Black horizontal bars highlight the time range of significant response differences (time-sliding one-way five-level ANOVA; see Materials and Methods). The colored windows mark the time range (defined in the FBA experiment) for which response averages are plotted on the right. Orange, blue, and green bar plots show window averages in the 110–150 ms, 205–275 ms, and 275–390 ms time range, respectively. The colored circles replot window averages of the FBA experiment (Fig. 3) for comparison. Error bars indicate SEM.

In sum, withdrawing attention from the target color circle while keeping the spatial focus of attention on the peripheral location of the circle preserved the response variation in early visual cortex as in Control Experiment 1, suggesting that the very initial response in V1 reflects sensory differences between probe colors. In contrast, later modulations in extrastriate visual cortex are small and inconsistent as in Control Experiment 1, indicating that the modulations seen in the FBA experiment beyond ~200 ms truly reflect the operation of FBA.

Although Control Experiment 2 clearly shows that the absence of the FBA-related response modulation is not due to a change of the spatial focus of attention, concerns could still be raised. Because the control experiments added items to the stimulus display, they did not exactly match the stimulus setup of the FBA experiment. This leaves the possibility that the added stimulation per se (in particular the RSVP stream) interfered with the response to the color items, which eventually obscured the response profile seen in the FBA experiment. Observations in a previous experiment, however, speak against this possibility (Bartsch, 2015, Experiment 2). In this experiment the experimental task and design was overall comparable to the FBA experiment. The experiment differed in that, aside from red and purple, a different set of probe colors was used and that probe color did not gradually vary in color distance to the target. Critically, an RSVP stream was presented together with the color circles as in Control Experiment 1, with subjects either performing the color or the RSVP task. For

the color task, a prominent FBA modulation appeared, which was effectively eliminated for the RSVP task, rendering it unlikely that the mere presence of the RSVP stream (as opposed to withdrawing FBA from the color target) in Control Experiment 1 is responsible for the absence of the modulation profile seen in the FBA experiment.

Discussion

Here, we show that attention to color is indexed by a sequence of modulations of the magnetic brain response that is generated in ventral extrastriate visual cortex. Analyzing the amplitude and time course of these modulations as a function of color distance to the target reveals that the response is initially coarsely selective for the target color (205–275 ms). Within the following ~100 ms, this selectivity increases, as indexed by a response attenuation of nontarget colors neighboring the target in color space. This coarse-to-fine change of selectivity over time is associated with a transition of the cortical locus of underlying modulations. Specifically, modulations showing coarse selectivity arise first in anterior ventral extrastriate areas (areas anterior to VO and lateral to PHC), whereas later sharpened selectivity develops in more posterior retinotopic visual areas (VO-1/hV4).

FBA modulates gain and tuning

The present findings demonstrate that FBA influences both gain and tuning of the feature-selective population response in visual cortex, an observation that aligns with interpretations of psychophysical experiments (Lee et al., 1999; Ling et al., 2009), as well as with observations made in brain-imaging studies (Murray and Wojciulik, 2004; Serences et al., 2009; Garcia et al., 2013). The present experiments extend this work by showing that gain and tuning arise from a dynamic coarse-to-fine selection process progressing from higher to lower hierarchical levels in visual cortex. Cortical selection in such a reverse hierarchical direction was reported previously to underlie spatial attention (Mehta et al., 2000; Hopf et al., 2006; Boehler et al., 2009; Lauritzen et al., 2009; Buffalo et al., 2010), as well as FBA to color and orientation (Bondarenko et al., 2012; Bartsch et al., 2015). These latter studies, however, did not clarify the role of reverse hierarchical selection for FBA. The present data suggest that it serves to sharpen selectivity for the attended feature, which is accomplished by propagating the locus of attentional selection to lower levels of representation, where the higher resolution of coding better aids discrimination (for a similar conclusion in the spatial domain, see Hopf et al., 2006).

Testing predictions of the ST model

The observed temporal order and hierarchical direction of FBA modulations fit key predictions of the ST model (Tsotsos et al., 1995; Tsotsos, 2011). ST proposes that the initial feedforward signal that passes through the visual cortical hierarchy is subject to task-dependent tuning (instruction to attend red). This preset tuning is only coarsely selective for the target (forward binding; Tsotsos et al., 2008) and the corresponding modulation of the population response reflects the contribution from a wide range of units more and less tuned to the target. Following this initial forward pass, a top-down winner-take-all process running in a reverse hierarchical direction within visual cortex prunes units less responsive to the target at progressively lower levels of representation (recurrence binding). This process increases the effective selectivity of units at higher levels because their response reflects the remaining input from lower-level units best responding to the target. ST makes several testable predictions: (1) FBA modulations should appear first at higher and then at lower levels of representation; (2) FBA modulations should show a time course of coarse-to-fine selectivity (Rothenstein and Tsotsos, 2014); and (3) because sharpened selectivity arises from a recurrent attenuation of less tuned units, there should be an overall attenuation of the response to nontarget colors instead of a selective enhancement of the target color, as proposed by some gain-field models (Salinas and Abbott, 1997). The present data provide support for all three predictions. Gain enhancements indexing coarse selectivity appeared in a region hierarchically higher than VO-1 and hV4. Subsequent modulations indexing sharper population tuning were maximal in VO-1/hV4. Over time, FBA was found to attenuate the response to color values away from the target instead of increasing the response to the target color. This is consistent with converging evidence for an FBA-driven attenuation of color values surrounding the target recently provided by an SSVEP experiment (Störmer and Alvarez, 2014). Furthermore, surround attenuation in the spatial domain has been reported to underlie the increasing resolution of discrimination in visual search (Boehler et al., 2009; Hopf et al., 2010).

It should be noted that the ST model was primarily developed with cortical problems of spatial coding in mind. Although an ST implementation has been formulated to account for the selection of features such as motion direction and velocity (Tsotsos, 2011), such a dedicated implementation does not yet exist for attention to color. A core feature of the ST model is that receptive fields with low spatial resolution at higher levels inherit the better resolution of smaller receptive fields from which they receive input. The hierarchy of color coding in visual cortex is not directly comparable to the coding hierarchy of space, not least because the spectral bandwidth of color cells was found to be approximately comparable at different hierarchical levels (de Monasterio and Schein, 1982; Desimone et al., 1985). For a realistic ST implementation of color selection, a better understanding of how color is hierarchically coded in visual cortex is needed. Regardless of the exact implementation, the delayed sharpening of population tuning toward lower-tier areas suggests a back-propagating attenuation of units less tuned to the attended color as proposed by the ST model.

Relation to the feature similarity gain (FSG) model

The FSG model (Treue and Martínez-Trujillo, 1999; Maunsell and Treue, 2006) is an account of FBA at the single-neuron level that primarily builds on observations in motion-selective area MT. Neurons in MT were shown to increase response gain if their direction preference aligned with the attended motion direction (Treue and Martínez-Trujillo, 1999). In contrast, neurons preferring directions far away from the attended one (anti-preferred direction) decreased their response below baseline. Although FBA typically does not change the tuning of individual units, the corresponding population response could show sharper tuning (Martínez-Trujillo and Treue, 2004; Treue and Martínez-Trujillo, 2006), as presently seen in the population color tuning of ventral extrastriate areas VO-1/hV4. For such a sharpening of population tuning to appear within the FSG framework, units tuned to antipreferred directions must attenuate their response below baseline. This attenuation could theoretically result from the elimination of forward projections of less tuned units, as suggested by the ST model. FSG, however, is not explicit about the hierarchical implementation of the modulatory effects. More research is needed to clarify how FSG's account of sharpened population tuning relates to the sharpening of color selectivity observed here.

Alternative accounts

The present data support the interpretation that the sharpening of color selectivity reflects the attenuation of less-tuned units. Alternatively, it is possible that individual color cells sharpen their tuning over time, which sums up to sharpened population tuning. Indeed, a dynamic change of selectivity has been reported in units coding for high-level features (Sugase et al., 1999; Hegdé and Van Essen, 2004, 2006; Ipata et al., 2012). In low-level feature-selective units, some increases of selectivity were reported (Spitzer et al., 1988). However, a dynamic change of selectivity has not been documented for color-selective units. Therefore, it is unlikely that a dynamic sharpening of the tuning of single units accounts for the delayed sharpening of the population response observed here. Of course, such a possibility cannot be ruled out because MEG recordings do not resolve responses at the level of single units.

Note Added in Proof: Figure 6*C* was incorrect in the Early Release version published September 25, 2017. The figure has now been corrected.

References

Amano K, Wandell BA, Dumoulin SO (2009) Visual field maps, population receptive field sizes, and visual field coverage in the human MT+ complex. J Neurophysiol 102:2704–2718. CrossRef Medline

Arcaro MJ, McMains SA, Singer BD, Kastner S (2009) Retinotopic organization of human ventral visual cortex. J Neurosci 29:10638–10652. CrossRef Medline

Bartsch M (2015) Determinants of global color-based attention: Insights from electromagnetic brain recording in humans. Doctoral dissertation, University of Magdeburg.

Bartsch MV, Boehler CN, Stoppel CM, Merkel C, Heinze HJ, Schoenfeld MA, Hopf JM (2015) Determinants of global color-based selection in human visual cortex. Cereb Cortex 25:2828–2841. CrossRef Medline

Boehler CN, Tsotsos JK, Schoenfeld MA, Heinze HJ, Hopf JM (2009) The center-surround profile of the focus of attention arises from recurrent processing in visual cortex. Cereb Cortex 19:982–991. CrossRef Medline

Bondarenko R, Boehler CN, Stoppel CM, Heinze HJ, Schoenfeld MA, Hopf JM (2012) Separable mechanisms underlying global feature-based attention. J Neurosci 32:15284–15295. CrossRef Medline

Brouwer GJ, Heeger DJ (2009) Decoding and reconstructing color from responses in human visual cortex. J Neurosci 29:13992–14003. CrossRef Medline

Buffalo EA, Fries P, Landman R, Liang H, Desimone R (2010) A backward progression of attentional effects in the ventral stream. Proc Natl Acad Sci U S A 107:361–365. CrossRef Medline

Chawla D, Rees G, Friston KJ (1999) The physiological basis of attentional modulation in extrastriate visual areas. Nat Neurosci 2:671–676. CrossRef Medline

Corbetta M, Miezin FM, Dobmeyer S, Shulman GL, Petersen SE (1990) Attentional modulation of neural processing of shape, color, and velocity in humans. Science 248:1556–1559. CrossRef Medline

Corbetta M, Miezin FM, Dobmeyer S, Shulman GL, Petersen SE (1991) Selective and divided attention during visual discriminations of shape, color, and speed: functional anatomy by positron emission tomography. J Neurosci 11:2383–2402. Medline

Cross EM, Chaffin WW (1982) Use of the binomial theorem in interpreting results of multiple test of significance. Educational and Psychological Measurement 42:25–34. CrossRef

Cutzu F, Tsotsos JK (2003) The selective tuning model of attention: psychophysical evidence for a suppressive annulus around an attended item. Vision Res 43:205–219. CrossRef Medline

de Monasterio FM, Schein SJ (1982) Spectral bandwidths of color-opponent cells of geniculocortical pathway of macaque monkeys. J Neurophysiol 47:214–224. Medline

Desimone R, Schein SJ, Moran J, Ungerleider LG (1985) Contour, color and shape analysis beyond the striate cortex. Vision Res 25:441–452. CrossRef Medline

Dumoulin SO, Wandell BA (2008) Population receptive field estimates in human visual cortex. Neuroimage 39:647–660. CrossRef Medline

Fuchs M, Wagner M, Köhler T, Wischmann HA (1999) Linear and nonlinear current density reconstructions. J Clin Neurophysiol 16:267–295. CrossRef Medline

Garcia JO, Srinivasan R, Serences JT (2013) Near-real-time feature-selective modulations in human cortex. Curr Biol 23:515–522. CrossRef Medline

Greene CA, Dumoulin SO, Harvey BM, Ress D (2014) Measurement of population receptive fields in human early visual cortex using back-projection tomography. J Vis 14:pii:17. CrossRef Medline

Guthrie D, Buchwald JS (1991) Significance testing of difference potentials. Psychophysiology 28:240–244. CrossRef Medline

Hegdé J, Van Essen DC (2004) Temporal dynamics of shape analysis in macaque visual area V2. J Neurophysiol 92:3030–3042. CrossRef Medline

Hegdé J, Van Essen DC (2006) Temporal dynamics of 2D and 3D shape representation in macaque visual area V4. Vis Neurosci 23:749–763. CrossRef Medline

Hopf JM, Luck SJ, Boelmans K, Schoenfeld MA, Boehler CN, Rieger J, Heinze HJ (2006) The neural site of attention matches the spatial scale of perception. J Neurosci 26:3532–3540. CrossRef Medline

Hopf JM, Boehler CN, Schoenfeld MA, Heinze HJ, Tsotsos JK (2010) The spatial profile of the focus of attention in visual search: Insights from MEG recordings. Vision Res 50:1312–1320. CrossRef Medline

Ipata AE, Gee AL, Goldberg ME (2012) Feature attention evokes task-specific pattern selectivity in V4 neurons. Proc Natl Acad Sci U S A 109:16778–16785. CrossRef Medline

Lauritzen TZ, D'Esposito M, Heeger DJ, Silver MA (2009) Top-down flow of visual spatial attention signals from parietal to occipital cortex. J Vis 9:18.1–18.14. CrossRef Medline

Lee BB, Martin PR, Valberg A (1988) The physiological basis of heterochromatic flicker photometry demonstrated in the ganglion cells of the macaque retina. J Physiol 404:323–347. CrossRef Medline

Lee DK, Itti L, Koch C, Braun J (1999) Attention activates winner-take-all competition among visual filters. Nat Neurosci 2:375–381. CrossRef Medline

Lee S, Papanikolaou A, Logothetis NK, Smirnakis SM, Keliris GA (2013) A new method for estimating population receptive field topography in visual cortex. Neuroimage 81:144–157. CrossRef Medline

Ling S, Liu T, Carrasco M (2009) How spatial and feature-based attention affect the gain and tuning of population responses. Vision Res 49:1194–1204. CrossRef Medline

Liu J, Wandell BA (2005) Specializations for chromatic and temporal signals in human visual cortex. J Neurosci 25:3459–3468. CrossRef Medline

Martínez-Trujillo JC, Treue S (2004) Feature-based attention increases the selectivity of population responses in primate visual cortex. Curr Biol 14:744–751. CrossRef Medline

Maunsell JH, Treue S (2006) Feature-based attention in visual cortex. Trends Neurosci 29:317–322. CrossRef Medline

McMains SA, Fehd HM, Emmanouil TA, Kastner S (2007) Mechanisms of feature- and space-based attention: response modulation and baseline increases. J Neurophysiol 98:2110–2121. CrossRef Medline

Mehta AD, Ulbert I, Schroeder CE (2000) Intermodal selective attention in monkeys. I: distribution and timing of effects across visual areas. Cereb Cortex 10:343–358. CrossRef Medline

Murray SO, Wojciulik E (2004) Attention increases neural selectivity in the human lateral occipital complex. Nat Neurosci 7:70–74. CrossRef Medline

Olshausen BA, Anderson CH, Van Essen DC (1993) A neurobiological model of visual attention and invariant pattern recognition based on dynamic routing of information. J Neurosci 13:4700–4719. Medline

Paltoglou AE, Neri P (2012) Attentional control of sensory tuning in human visual perception. J Neurophysiol 107:1260–1274. CrossRef Medline

Rothenstein AL, Tsotsos JK (2014) Attentional modulation and selection: an integrated approach. PLoS One 9:e99681. CrossRef Medline

Rousseeuw PJ (1987) Silhouettes: a graphical aid to the interpretation and validation of cluster analysis. Journal of Computational and Applied Mathematics 20:53–65. CrossRef

Sàenz M, Buraĉas GT, Boynton GM (2002) Global effects of feature-based attention in human visual cortex. Nat Neurosci 5:631–632. CrossRef Medline

Salinas E, Abbott LF (1997) Invariant visual responses from attentional gain fields. J Neurophysiol 77:3267–3272. Medline

Serences JT, Saproo S, Scolari M, Ho T, Muftuler LT (2009) Estimating the influence of attention on population codes in human visual cortex

using voxel-based tuning functions. Neuroimage 44:223–231. CrossRef Medline

Spitzer H, Desimone R, Moran J (1988) Increased attention enhances both behavioral and neuronal performance. Science 240:338–340. CrossRef Medline

Störmer VS, Alvarez GA (2014) Feature-based attention elicits surround suppression in feature space. Curr Biol 24:1985–1988. CrossRef Medline

Sugase Y, Yamane S, Ueno S, Kawano K (1999) Global and fine information coded by single neurons in the temporal visual cortex. Nature 400:869–873. CrossRef Medline

Treue S, Martínez-Trujillo J (2006) Visual search and single-cell electrophysiology of attention: Area MT, from sensation to perception. Visual Cognition 14:898–910. CrossRef

Treue S, Martínez-Trujillo JC (1999) Feature-based attention influences motion processing gain in macaque visual cortex. Nature 399:575–579. CrossRef Medline

Tsotsos JK (1990) Analyzing vision at the complexity level. Behav Brain Sci 13:423–469. CrossRef

Tsotsos JK (2011) A computational perspective on visual attention. Cambridge, MA: MIT.

Tsotsos JK, Culhane SM, Wai WYK, Lai Y, Davis N, Nuflo F (1995) Modeling visual attention via selective tuning. Artificial Intelligence 78:507–545. CrossRef

Tsotsos JK, Rodríguez-Sánchez AJ, Rothenstein AL, Simine E (2008) The different stages of visual recognition need different attentional binding strategies. Brain Res 1225:119–132. CrossRef Medline

Wade AR, Brewer AA, Rieger JW, Wandell BA (2002) Functional measurements of human ventral occipital cortex: retinotopy and colour. Philos Trans R Soc Lond B Biol Sci 357:963–973. CrossRef Medline

Wang L, Mruczek RE, Arcaro MJ, Kastner S (2015) Probabilistic maps of visual topography in human cortex. Cereb Cortex 25:3911–3931. CrossRef Medline